Proton dynamics in $Rb_3H(SO_4)_2$ doped with Mn^{2+} studied by EPR and impedance spectroscopy

2009 J. Phys.: Condens. Matter 21 205401

(http://iopscience.iop.org/0953-8984/21/20/205401)

J. Phys.: Condens. Matter **21** (2009) 205401 (6pp) doi:10.1088/0953-8984/21/20/205401

Proton dynamics in $Rb_3H(SO_4)_2$ doped with Mn^{2+} studied by EPR and impedance spectroscopy

A Ostrowski[1] **and W Bednarski**

Institute of Molecular Physics, Polish Academy of Sciences, M Smoluchowskiego 17, PL-60-179 Poznań, Poland

E-mail: ostrowski@ifmpan.poznan.pl

Received 12 November 2008, in final form 17 March 2009
Published 8 April 2009
Online at stacks.iop.org/JPhysCM/21/205401

Abstract

The temperature dependence of the linewidth ΔB_{pp} and spin Hamiltonian parameters of $Rb_3H(SO_4)_2$ (RHS) crystals were studied by X-band continuous-wave electron paramagnetic resonance. Direction cosines of the zero-field-splitting (ZFS) tensor and the coordination of the Mn^{2+} impurities in the crystal lattice were determined in the temperature range 20–450 K. The EPR spectra of crystalline samples and their irreversible changes into pseudo-powder spectra after heating above the superprotonic phase transition temperature were found. Our studies of electric conductivity have shown that, for crystals doped with Mn^{2+} ions, the conductivity values increase after heating by about one order of magnitude at intermediate temperatures (below the transition temperature to the superionic phase) in comparison with those of the pure RHS.

1. Introduction

The $M_3H(XO_4)_2$ crystal family, where M = NH_4, Rb, K, Cs; X = S, Se, reveals many interesting properties related to phase transitions, especially a high proton conductivity [1–3]. In particular, the protonic conductivity of $Rb_3H(SO_4)_2$ (RHS) reaches values of the order of 10^{-2} Ω^{-1} cm^{-1} above the temperature $T_s \sim 490$ K of the superionic phase transition [3]. At room temperature RHS belongs to the space group $C2/c$, $Z = 4$ with lattice parameters $a = 15.144(3)$, $b = 5.890(3)$, $c = 10.149(1)$ Å and $\beta = 102.55(1)^\circ$ [4]. There are two sets of rubidium ions in the RHS structure. The rubidium ions Rb(I) of the first class are placed at general positions, whereas the Rb(II) ions of the second class reside at special positions on the twofold axis.

The superprotonic properties of most $M_3H(XO_4)_2$ materials are directly related to the ferroelastic/paraelastic phase transitions [3, 5, 6] and are accompanied by symmetry changes from the point group $2/m$ to the $\bar{3}m$ one. The superprotonic phase of the $Rb_3H(SO_4)_2$ crystal structure is still unknown. Pawlowski *et al* [3] reported that RHS undergoes an irreversible phase transition and transforms into a polycrystalline state at a temperature T_s. The authors suggest that RHS is a non-ferroelastic crystal; however, below T_s a twin structure was observed [3]. On the other hand, the temperature dependences of the optical polarizing microscopy images and the stress–strain hysteresis curve measurements of non-annealed crystal show that domain boundaries are altered easily by the application of very weak mechanical stresses. The ferroelastic domain switching stress of $Rb_3H(SO_4)_2$ crystals (0.7 MPa) has been found [5]. Moreover, x-ray powder diffraction measurements under moderate humidification performed by Cowan *et al* [7] show peaks that can be attributed to Rb_2SO_4 and an unknown solid phase. The results indicate that the $Rb_3H(SO_4)_2$ conductivity increase corresponds to a solid state disproportionation rather than to a polymorphic transition. The former is described as $Rb_3H(SO_4)_2(s) \rightarrow Rb_2SO_4(s) + Rb_mH_n(SO_4)_p(s)$ (with $p = (m+n)/2$), where the phase with unknown composition is richer in sulfuric acid with respect to $Rb_3H(SO_4)_2$. It has been proposed that the unknown phase, possibly $Rb_5H_3(SO_4)_4$, is superprotonic in nature [7].

Paramagnetic Mn^{2+} ions have been chosen as a dopant because, with the help of its EPR spectra, one could control the concentration and coordination of the impurities in the

[1] Author to whom any correspondence should be addressed.

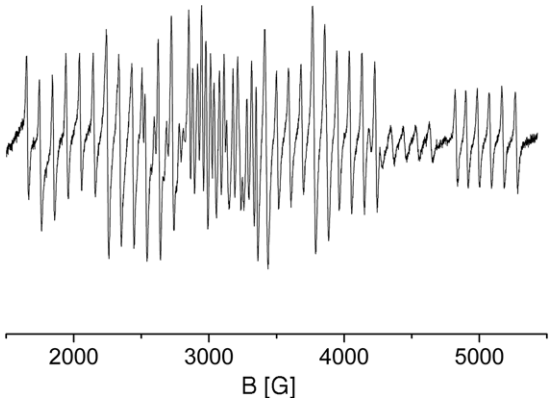

Figure 1. The EPR spectrum of the single-domain $Rb_3H(SO_4)_2$:Mn^{2+} crystal at room temperature. An external magnetic field B is parallel to the y–ZFS tensor axis.

crystal structure. The EPR spectra monitoring before and after annealing allows one to control the structural stability.

In the current work we have carried out EPR measurements in a wide range of temperatures, including that of the superprotonic phase transition. In addition, we have performed impedance spectroscopy measurements to inspect the influence of Mn^{2+} impurities on the conductivity and temperature of the superprotonic phase transition.

2. Experimental details

Hexagonal plate-like $Rb_3H(SO_4)_2$ crystals were grown isothermally at 295 K from an aqueous solution containing Rb_2SO_4 and H_2SO_4 in stoichiometric ratio and a small amount of $MnSO_4{\cdot}4H_2O$ (0.3 wt% of the solution). An optical investigation of the single crystal in polarized light at room temperature (RT) reveals a ferroelastic $n \cdot 60^\circ$ domain pattern.

Conductivity and dielectric measurements were carried out with 4284A Hewlett Packard (20 Hz–1 MHz) and 4285A Agilent (75 kHz–30 MHz) Precision LCR Meters. The temperature was controlled and stabilized with the LakeShore 340 Temperature Controller. The polycrystalline samples were prepared by mechanical grinding of monocrystals in a mortar and then pressed at 150 MPa into pellets (of 8 mm diameter and 1.5–2.0 mm thickness). Subsequently, the silver electrodes were deposited on the pellets and on the (100) plane of a single-domain crystal sample. The conductivity measurements were performed at a heating/cooling rate of 1 K min^{-1} in the temperature range (295–510) K in a dry nitrogen and a water-saturated nitrogen gas ($N_2 + H_2O$) environment.

The EPR spectra of single-domain samples were recorded with a Bruker ELEXSYS X-band spectrometer. The temperature was controlled and stabilized with a BVT3000 Bruker Temperature Controller or ITC 503s Oxford Temperature Controller. The EPR measurements were performed in a gaseous nitrogen or helium atmosphere.

In order to determine the Mn^{2+} concentration in the samples, the spectra were double-integrated and compared with the intensity of a standard.

Table 1. Spin Hamiltonian parameters and direction cosines of the ZFS tensor of Mn^{2+} complexes in $Rb_3H(SO_4)_2$ at RT.

g_{iso}	$A_\parallel$ (G)	$A_\perp$ (G)	D (G)	E (G)	$(a\text{-}F)$ (G)
1.997(3)	−95(1)	−94(1)	667(5)	62(3)	19(1)
Direction cosines of the main axes of the ZFS tensor XYZ					
x	±0.570	0.662	∓0.487		
y	∓0.564	0.746	±0.354		
z	±0.597	0.073	±0.799		

3. Results

3.1. EPR spectra at RT

The XYZ orthogonal laboratory frame chosen for the EPR anisotropy measurement was related to the $\vec{a}$, $\vec{b}$ and $\vec{c}$ crystallographic axes as follows: $\vec{X} \parallel \vec{c}$, $\vec{Y} \parallel \vec{b}$ and $\vec{Z} \parallel \vec{a}^* = \vec{c} \times \vec{b}$. Figure 1 shows the EPR spectrum with an external magnetic field B parallel to the y—zero-field-splitting (ZFS) tensor—axis. Due to the point symmetry $2/m$ there are two structurally non-equivalent Mn^{2+} complexes (different direction cosines) at room temperature in the single-domain crystal (table 1). The concentration of Mn^{2+} ions in RHS was about 5000 ppm.

The EPR spectrum of an Mn^{2+} centre is described by the spin Hamiltonian [8, 9]:

$$H = g_{iso}\beta\vec{B}\hat{\vec{S}} + B_2^0O_2^0 + B_2^2O_2^2 + B_4^0O_4^0 + B_4^4O_4^4 + A_\parallel\hat{S}_z\hat{I}_z + A_\perp(\hat{S}_x\hat{I}_x + \hat{S}_y\hat{I}_y), \quad (1)$$

where O_n^m are the extended Stevens operators, B_n^m are the zero-field-splitting parameters, and $A_\parallel$ and $A_\perp$ are the hyperfine structure tensor components. The common zero-field-splitting parameters: axial—D, non-axial—E and the conventional high-spin operator parameters F and a are related to the coefficients B_n^m:$3B_2^0 = D$, $B_2^2 = E$, $B_4^0 = \frac{1}{120}a + \frac{1}{180}F$ and $B_4^4 = \frac{1}{24}a$.

The values of the spin Hamiltonian parameters and direction cosines at RT are collected in table 1.

Similarly as for the $K_3H(SO_4)_2$ and $(NH_4)_3H(SO_4)_2$ crystals [10, 11], the direction cosines indicate the same mechanism of the excess charge compensation. In the $Rb_3H(SO_4)_2$ crystals the Mn^{2+} ion replaces the Rb^+(I) ion and its positive excess charge is compensated by a proton vacancy. The Mn^{2+} ion coordinates with six non-uniform distant oxygen atoms of neighbouring SO_4 groups which form a distorted octahedron. Figures 2(A) and (B) present the structure of RHS and coordination of Mn^{2+}, respectively.

3.2. Conductivity studies

Figure 3 presents the Arrhenius plots of the proton conductivity σ in pure and Mn^{2+}-doped RHS pellets and monocrystals measured along the a^* axis during heating/cooling cycles. The measurements on pellets were performed in a water-saturated nitrogen gas ($N_2 + H_2O$) environment in order to prevent samples from dehydration [7].

Above about 480 K, the conductivity significantly increases and reaches the same value for all measured samples.

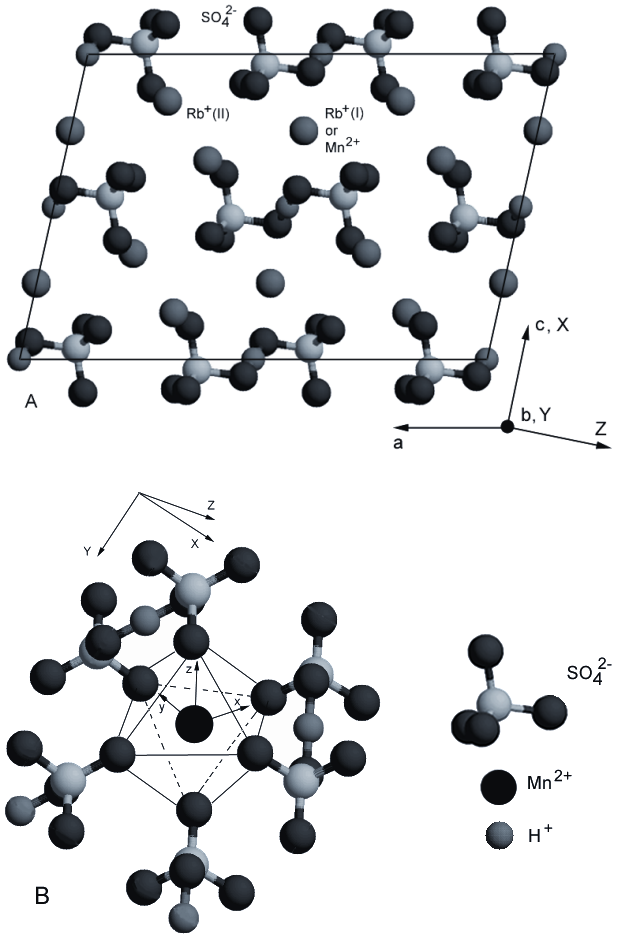

Figure 2. The crystal structure of $Rb_3H(SO_4)_2$ at room temperature (A) and distorted octahedral coordination neighbourhood of Mn^{2+} formed by six oxygen ions from six neighbouring SO_4 groups (B).

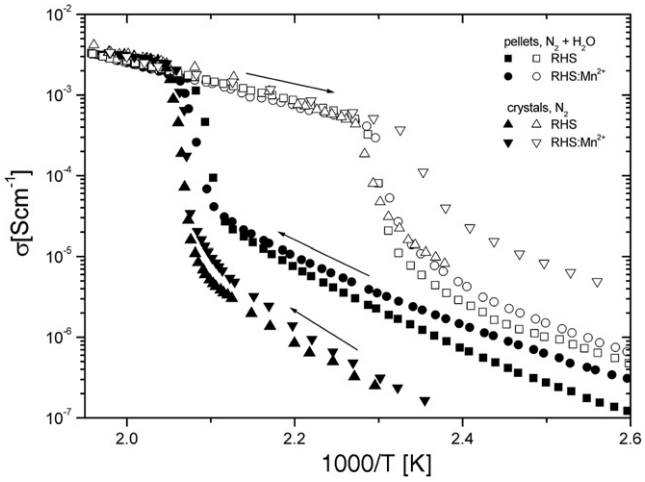

Figure 3. Temperature dependences of the conductivity of pure and Mn^{2+}-doped (5000 ppm) $Rb_3H(SO_4)_2$ pellets and crystals measured along the a^* axis in an atmosphere of dry N_2 and with H_2O partial pressure of about 0.5 mol% in the N_2 gas.

The activation energy value for pure as well as doped pellets and crystals in the superprotonic phase is similar, i.e. 0.67(0.01) eV. On cooling, a significant thermal hysteresis

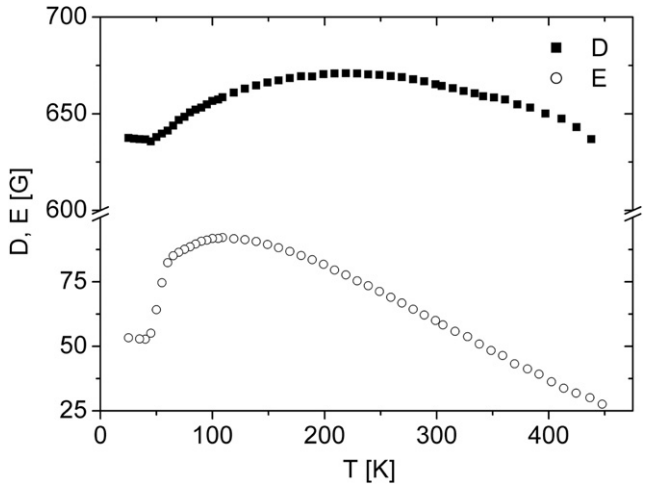

Figure 4. Temperature dependence of D and E zero-field-splitting parameters of Mn^{2+} in an $Rb_3H(SO_4)_2$ crystal.

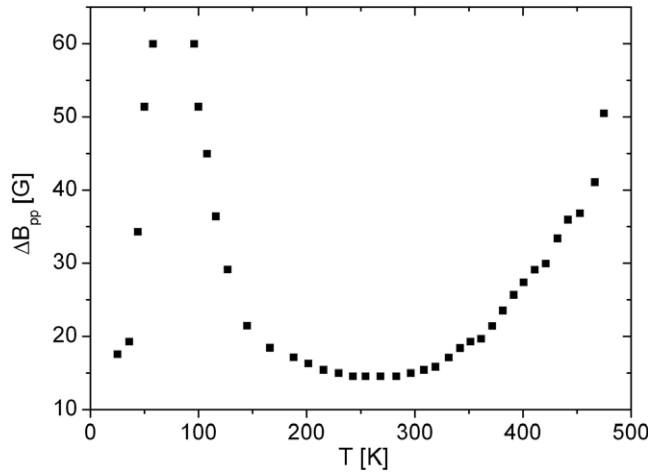

Figure 5. Temperature dependence of the ΔB_{pp} linewidth of the $(M_s = 5/2, m = -5/2) \leftrightarrow (M_s = 3/2, m = -5/2)$ transition in $Rb_3H(SO_4)_2$:Mn^{2+}.

occurs, especially for Mn^{2+}-doped crystal samples. After cooling at the intermediate phase the Mn^{2+}-doped crystal reveals a conductivity higher by about one order of magnitude in comparison to pure RHS.

3.3. Linewidth and spin Hamiltonian parameters versus temperature

Figure 4 presents the D and E zero-field-splitting parameters in the temperature range of 20–450 K. The D parameter increases with temperature increasing to 220 K and then decreases at higher temperatures. At about 110 K the E parameter reaches a maximum value and further linearly decreases. Such a behaviour of both parameters, i.e. the lowering of the E/D ratio, indicates that the deviation of the local axial symmetry of the Mn^{2+} complex decreases with temperature.

Figure 5 shows the temperature dependences of ΔB_{pp} linewidth (the distance between the inflection points of the

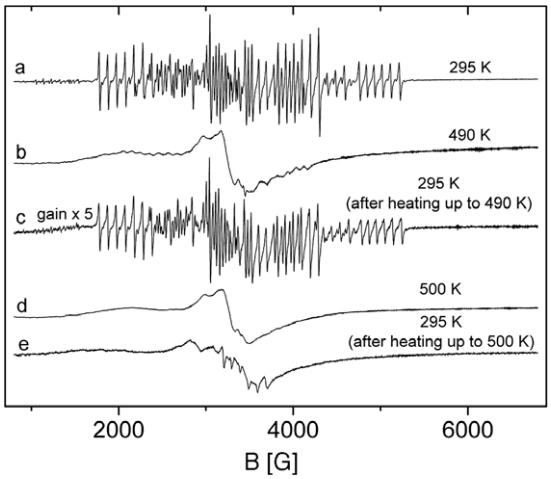

Figure 6. EPR spectra of the single-domain $Rb_3H(SO_4)_2$:Mn^{2+} crystal recorded at 295 K (a), 490 K (b), 295 K after heating up to 490 K (c), 500 K (d) and 295 K after heating up to 500 K (e). An external magnetic field: $B \perp a^*$, $\langle(B, b) = 15°$.

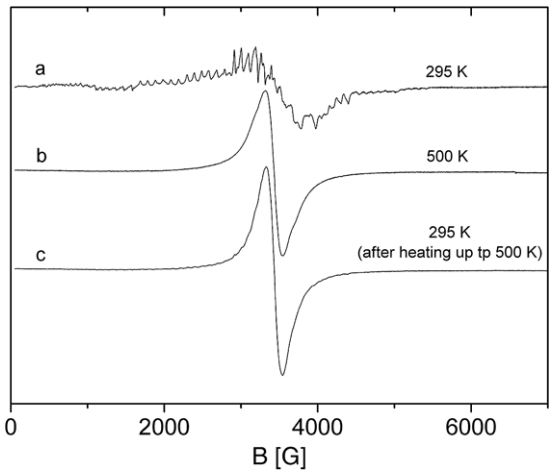

Figure 7. EPR spectra of powdered $Rb_3H(SO_4)_2$:Mn^{2+} at 295 K (a), 500 K (b) and at 295 K after heating up to 500 K (c).

EPR line absorption) for the ($M_s = 5/2$, $m = -5/2$) $\leftrightarrow$ ($M_s = 3/2$, $m = -5/2$) transition in the temperature range of 25–475 K. A similar ΔB_{pp} temperature dependence was recorded in our previous EPR measurements on the isomorphous $K_3H(SO_4)_2$ crystal [10, 12] and will be discussed below.

3.4. EPR spectra below and above the superprotonic phase transition

The temperature evolution of the EPR spectra of the single-domain RHS:Mn^{2+} crystal is shown in figure 6. Each spectrum was recorded at a temperature indicated in the figure after heating/cooling at a constant rate of 50 K min^{-1}. Such a fast heating/cooling rate has been chosen in order to inhibit the sample dehydration. In this way, we were able to find a temperature at which irreversible changes of EPR spectra might have occurred. Any changes in the EPR spectra at room temperature for the samples heated up to 480 K were not recorded. After heating up to 490 K, the intensity of the narrow lines in the EPR spectrum decreases about five times and the broad line in the central part of the spectrum appears (figure 6(c)). Figure 6(e) shows the EPR spectrum of the sample annealed at 500 K and recorded at 295 K. Such an EPR spectrum may be called a pseudo-powder one (see below). Although the broad isotropic line is predominant in the latter EPR spectrum due to its intensity, some anisotropy of the narrow lines is still observable.

Figure 7 shows the EPR spectra of powdered samples of RHS:Mn^{2+} recorded at 295 K (a), 500 K (b) and at 295 K after heating up to 500 K (c). After heating up to 500 K, a single broad line ($\Delta B_{pp} \sim 210$ G) has been recorded at room temperature. An irreversible change of the EPR spectrum has been observed, similarly as for crystalline samples.

4. Discussion and conclusion

The proton transport, which leads to high electrical conductivity in the $M_3H(XO_4)_2$ family, is currently described by several theoretical models based mainly on the two-step Grotthus mechanism. According to these models, the proton is transferred within hydrogen bonds of the $XO_4 \cdots H - -XO_4$ dimer (intra-bond motion), followed by a proton jumping between neighbouring XO_4 tetrahedra (inter-bond motion) [13–17]. The proton transport is correlated with a rapid reorientation of XO_4 groups and a temperature increase enhances the XO_4 reorientation as well as the proton jump rate in the double-well potential [18]. As mentioned above, the Mn^{2+} ion is coordinated with six neighbouring SO_4 groups and requires a proton vacancy. This is why the changes in the Mn^{2+} EPR spectra should be related to the proton/proton vacancy and SO_4 group dynamics.

The ΔB_{pp} linewidth minima at about 260 K in Mn-doped $Rb_3H(SO_4)_2$ crystals and in Mn-doped $K_3H(SO_4)_2$ result from the effect of crystal field fluctuations on the Mn^{2+} complex due to the correlation between the 'inter-' and 'intra-bond' motion of protons [10, 12].

With increasing temperature the inter-bond motion frequency increases, which leads to resonance line broadening. Similar results were previously reported by Dolinšek *et al* [18]. A deuteron two-dimensional exchange NMR experiment has shown that the deuteron inter-bond motion has already been observed at room temperature as a precursor of superionic conductivity.

At about 85 K a significant ΔB_{pp} linewidth broadening can be observed. Such a line anomaly is usually observed close to the temperature of the phase transition. In contrast to $Rb_3D(SO_4)_2$, the compound $Rb_3H(SO_4)_2$ [18] does not undergo a ferroic phase transition. There is a question: does Mn^{2+} doping of the $Rb_3H(SO_4)_2$ crystal evoke a bulk phase transition similar to that observed in the deuterated crystal? After comparison of the $\varepsilon'(T)$ data (figure 8) for $Rb_3D(SO_4)_2$, $Rb_3H(SO_4)_2$ and $Rb_3H(SO_4)_2$:Mn^{2+} one finds that the answer is negative. Finally, the low temperature ΔB_{pp} linewidth

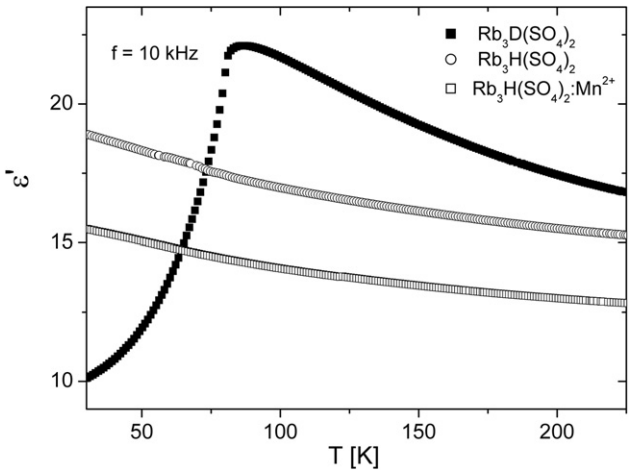

Figure 8. Temperature dependence of the real parts ε' of the complex dielectric constants for $Rb_3D(SO_4)_2$, $Rb_3H(SO_4)_2$ and $Rb_3H(SO_4)_2$:Mn^{2+} crystals measured along the a^* axis. Measurements were performed for non-annealed samples in a gaseous helium atmosphere.

anomaly around 85 K (observed also in $K_3H(SO_4)_2$ [10]) is attributed [19] to the presence of a 'local mode' strongly coupled to protons, as predicted by Yamada [20].

The analysis of the EPR spectra recorded at room temperature for crystalline and powdered samples, previously heated up to 500 K, indicates that the phase transition in $Rb_3H(SO_4)_2$ is irreversible. It can be observed that the EPR spectra of the crystalline sample after annealing (figure 6(e)) is similar to that of the non-annealed powdered sample (figure 7(a)). Although a slight anisotropy of EPR resonance lines was still observed for the annealed crystal, it can be admitted that the EPR spectrum presented in figure 6(e) is of a pseudo-powder character and results from a wide distribution of the spin Hamiltonian parameters.

A pseudo-powder spectrum is defined as a spectrum which consists of many spectra with different spin Hamiltonian parameters. Experimentally, one has to do with spectra of crystalline, and not powdered, samples. These spectra show a broad predominant isotropic line of high intensity with some less intense lines showing traces of anisotropy. Unfortunately, in practice the latter cannot be attributable to well-defined spin Hamiltonians, since one should expect that the sets of the spin Hamiltonian parameters for different components undergo variations after annealing and become unknown, although they likely originate from different known components such as Rb_2SO_4:Mn^{2+}, $Rb_2S_2O_7$:Mn^{2+}, $Rb_5H_3(SO_4)_4$:Mn^{2+}, etc, formed during the annealing process, as proposed by Cowan *et al* [7].

In addition, we expect very strong motional effects at high temperatures and thus any simulation of EPR spectra would be very speculative. In conclusion, a powder sample does not reveal any line position anisotropy nor EPR spectrum shape for different orientation of the magnetic field by definition. In the case of a pseudo-powder sample the anisotropy line position versus magnetic field orientation is very weak and in our case is mainly limited only to the lineshape changes versus magnetic field orientation.

In general, for the $M_3H(XO_4)_2$ crystal family a huge anisotropy of the conductivity below and above the phase transition temperature was recorded and is seen to be strictly related to the crystal structure, especially to the hydrogen bond arrangement [2]. For this reason, powdered samples reveal conductivity comparable to that of the crystalline samples in the plane of the hydrogen bond, where the highest conductivity occurs [2, 7, 21, 22]. This results from averaging over grain orientations in polycrystalline samples. A comparison of conductivity data of RHS crystals and powdered samples clearly shows that annealing leads to isotropic conductivity above T_s in pure and doped RHS samples.

Our EPR and conductivity measurements show that the superprotonic phase transition in RHS is irreversible, as previously reported by Cowan *et al* [7]. We suppose that pseudo-powder EPR spectra result from a distribution of spin Hamiltonian parameters. Isotropic conductivity recorded after annealing indicates that the new superprotonic phase reveals a huge disorder in the crystal lattice and hydrogen bonds. In addition, the doping of RHS with Mn^{2+} (5000 ppm) increases the number of proton vacancies, which ultimately leads to an increase in conductivity in the intermediate phase, similar to that observed by us for the $(NH_4)_3H(SO_4)_2$:Mn^{2+} superprotonic conductor [22].

Acknowledgments

This work has been supported by the Polish Ministry of Education and Science with a grant in the period of 2005–2008 under Programme no. PO3B 032 29.

We would like to thank Professors S Waplak and A R Ferchmin for discussions and J Janakowski for his help in part of the EPR measurements.

References

[1] Baranov A I 2003 *Kristallografija* **48** 1081
[2] Kamimura H, Matsuo Y, Ikehata S, Ito T, Komukae M and Osaka T 2004 *Phys. Status Solidi* b **241** 61
[3] Pawlowski A and Polomska M 2005 *Solid State Ion.* **176** 2045
[4] Fortier S, Fraser M E and Heyding R D 1985 *Acta Crystallogr.* C **41** 1139
[5] Lim A R, Nam S W, Chang J H and Jeong S Y 2006 *J. Appl. Phys.* **99** 54102
[6] Hatori J, Matsuo Y and Ikehata S 2006 *Solid State Commun.* **140** 452
[7] Cowan L A, Morcos R M, Hatada N, Navrotsky A and Haile S M 2008 *Solid State Ion.* **179** 305
[8] Jain V K and Lehmann G 1990 *Phys. Status Solidi* b **159** 495
[9] Rudowicz C, Gnutek P and Budzyński P 2008 *J. Phys.: Condens. Matter* **20** 295219
[10] Ostrowski A and Krupska A 2006 *Phase Transit.* **79** 569
[11] Bednarski W and Waplak S 1997 *Acta Phys. Pol.* A **90** 1185
[12] Waplak S 1994 *Acta Phys. Pol.* A **86** 939
[13] Haile S M 2003 *Acta Mater.* **51** 5981
[14] Pavlenko N I and Stasyuk I 2001 *J. Phys.: Condens. Matter* **13** 4081
[15] Pavlenko N I and Stasyuk I V 2001 *J. Chem. Phys.* **114** 4607
[16] Kamimura H and Watanabe S 2001 *Phil. Mag.* B **81** 1011
[17] Ito T and Kamimura H 1998 *J. Phys. Soc. Japan* **67** 1999
[18] Dolinšek J, Mikac U, Javoršek J E, Lahajnar G, Blinc R and Kirpichnikova L F 1998 *Phys. Rev.* B **58** 8445

[19] Bednarski W, Ostrowski A and Waplak S 2008 *Solid State Commun.* **146** 365
[20] Yamada Y 1995 *Ferroelectrics* **170** 23
[21] Chisholm C R I and Haile S M 2001 *Solid State Ion.* **145** 179
[22] Bednarski W, Ostrowski A and Waplak S 2008 *Solid State Ion.* **179** 1974